



OPEN

# Chemical mechanical polishing as an alternative surface treatment technique for corrosion prevention of carbon steel in an acidic medium

Mohamed Ahmed<sup>1✉</sup>, Buthainah Ali Al-Timimi<sup>2,3✉</sup>, Maha Al-Ali<sup>4</sup>, Ghassan H. Abdullah<sup>4</sup>, Safa Khalaf Atiyaha<sup>5</sup>, Ahmed Yaseen Ali Aljanabi<sup>6</sup> & Maizirwan Mel<sup>3</sup>

Chemical mechanical polishing (CMP) has been a standard technique in semiconductor manufacturing for achieving smooth surfaces. CMP utilizes a synergistic interplay of chemical and mechanical interactions to achieve the desired removal rates, selectivity, and ultimately planarity with different substrate materials. In this study, the impact of CMP on the surface properties of steel used in the petroleum industry was examined, with a focus on its corrosion behavior posttreatment. Steel samples were subjected to CMP with and without an oxidizer in a silica-based slurry, and their surface characteristics were compared to those of samples polished mechanically. The addition of an oxidizer to the slurry resulted in increased material removal rates and the formation of an oxide layer on the surface; this phenomenon was not observed in CMP without an oxidizer. However, in mechanical polishing, the action of silicon carbide grains on the steel surface led to an increase in the removal rate but caused a decrease in its corrosion resistance. Compared with other treatments, the oxide layer provided a good protective barrier against corrosion and improved the corrosion resistance of the steel substrate. Based on the results from the practical study, an improvement in the corrosion resistance properties was observed due to the chemical reaction of the oxidizer and the mechanical action of the silica nanoparticles; these results showed the importance of chemical mechanical polishing as an alternative method to reduce the corrosion of steel in acidic environments. Additionally, the effect of hydrogen peroxide in a silica slurry with respect to the wettability, surface roughness, and hardness of steel was examined using contact angle measurements, profilometry, scanning electron microscopy, and microhardness tests.

**Keywords** Chemical mechanical polishing, Immersion test, Electrochemical corrosion test, Hydrogen peroxide oxidizer, Silica-based slurry, Surface roughness, Contact angle, Material removal rate

## Abbreviations

CMP	Chemical mechanical polishing
MP	Mechanical polishing
H <sub>2</sub> O <sub>2</sub>	Hydrogen peroxide
SiO <sub>2</sub>	Silicon dioxide (Silica)
MRR	Material removal rate
Ra	Average surface roughness
SEM	Scanning electron microscopy
DIW	Deionized water
SCE	Saturated calomel electrode
E <sub>corr</sub>	Corrosion potential

<sup>1</sup>Mechanical Engineering Department, College of Engineering, Tikrit University, Tikrit, Iraq. <sup>2</sup>Chemical Engineering Department, University of Technology-Iraq, Baghdad, Iraq. <sup>3</sup>Chemical Engineering and Sustainability Department, Faculty of Engineering, International Islamic University of Malaysia (IIUM), Kuala Lumpur, Malaysia. <sup>4</sup>Oil and Gas Refining Engineering Department, College of Petroleum Process Engineering, Tikrit University, Tikrit, Iraq. <sup>5</sup>Petroleum Systems Control Engineering Department, College of Petroleum Processes Engineering, Tikrit University, Tikrit, Iraq. <sup>6</sup>Modeling and Design Program, Atilim University, Ankara, Turkey. ✉email: mohammed.ahmed72@tu.edu.iq; buthainah.a.abed@uotechnology.edu.iq

$I_{\text{corr}}$	Corrosion current density
$\beta_A$	Anodic Tafel Slope
$\beta_C$	Cathodic Tafel Slope
CR	Corrosion rate
Tc	Corrosion rate in mm/year
EW	Equivalent weight
MRP	Material removal process
pH	Potential of hydrogen (Acidity/Alkalinity Measure)

The surface properties of materials can influence how they can be joined, painted, and functionalized and how they respond to aggressive environments, such as corrosive environments. Surface conditions determine the formation of passive/protective layers on a surface in different environments and consequently affect the chemical response of a material, such as in the case of corrosion<sup>1</sup>. The investigation of the electrochemical properties of carbon steel has been the focus of several studies for a variety of applications in different industries, such as storage tanks, construction materials for chemical reactors, boilers and heat exchangers and oil and gas transport pipelines<sup>2,3</sup>. Mechanical treatments of the surface alter the surface properties by changing the arrangements of atoms in the surface plane<sup>4</sup>. Mechanical surface treatment induces subsurface alterations marked by macroscopic imperfections, such as roughness, abrasion, and scratches<sup>5,6</sup>. Furthermore, it results in localized dissipation of energy and matter, accompanied by an inadequately regulated temperature rise and subsequent cooling; these factors partially contribute to the significant residual compressive stress<sup>7–9</sup>. Dynamic recrystallization occurs because of significant deformation and localized temperature elevation, resulting in a nanostructured configuration known as a grain layer<sup>8,10</sup>. These surface alterations can affect the local characteristics of the material and the reactivity of the steel<sup>11</sup>. As a result, these alterations can cause adverse changes to the passive layer generated on the steel, reducing its corrosion and stress corrosion cracking resistance<sup>10–13</sup>. A surface can be treated chemically<sup>14</sup>, mechanically<sup>15,16</sup>, or by a combination of the two<sup>17,18</sup>. Commonly used mechanical surface treatment methods include polishing, grinding, pressure abrasive cleaning, buffing and brush cleaning.

Chemical mechanical polishing (CMP) is a wet polishing process that uses a combination of mechanical and chemical actions to achieve global planarity on a surface<sup>19–23</sup>. Different from traditional surface treatments with harsh oxidation chemicals, the CMP method provides the option to regulate the nanometer-level roughness and is a straightforward process involving a rotating machine, pad, and slurry with harder powder than the film being treated<sup>24</sup>. This method is notably more environmentally friendly than many other chemical treatment methods. The substances used in this CMP process do not have a significant impact on the environment. Because this approach is more environmentally friendly than other chemical treatments, it can minimize the negative impact on the environment during the large-scale production of solar panels. Because of these advantages, CMP has been utilized by the manufacturing sector for semiconductor production processes, including integrated circuits (ICs) and electronic devices, for many years<sup>25–27</sup>.

Lei and Luo prepared spherical SiO<sub>2</sub> and examined its effectiveness in polishing hard disks. Their experimental findings demonstrated an increase in polishing performance<sup>28</sup>. Seo and Lee suggested that the CMP process involved the sequential formation of a passive layer by the oxidizer and abrasion by abrasives in the slurry. Nonetheless, achieving balanced etching and passivation reactions is needed to prevent a rapid etching rate and ensure high overall surface planarity<sup>29</sup>. Hu used a silica nanoparticle-based slurry, studied the effects of the oxidizer and pH on the polishing performance of stainless steel and reported that elevated material removal rates (MRRs) were essential for oxidation to occur in an acidic slurry<sup>30</sup>. However, the formation of microdefects ranging from 1 to 2 µm in size was inevitably observed on the post-CMP surfaces. In a study by Lee et al. the electrochemical mechanical polishing (ECMP) technique was utilized for polishing stainless steel substrates. During ECMP, an additional anodic potential was applied to the substrate, i.e., stainless steel, and after polishing, a reduced surface roughness (23 nm) was observed with respect to that of the post-CMP surface roughness (38 nm)<sup>31</sup>.

The basic mechanism of the CMP process is the mechanical removal of the chemically softened material surface<sup>32</sup>. The main components of a CMP process/system are the substrate, polishing pad, and slurry. In addition, the chemicals in the slurry react with the metal surface and form an oxide layer, whereas the presence of abrasive nano/microparticles on the pad surface removes the material on the wafer surface. During this process, the depassivated areas dissolve until the passive oxide layer forms again<sup>33–36</sup>. Many studies suggest that the presence of oxidizers in slurries enhances the material removal rates. The most extensively used oxidizer during CMP is hydrogen peroxide (H<sub>2</sub>O<sub>2</sub>) because of its high stability and strong oxidizing ability<sup>37–39</sup>. The effects of different sizes of colloidal silica nanoparticles and their efficacy on 52,100 steel were examined by Keo et al.<sup>40</sup>. They reported that a smooth surface with a low surface roughness near 8.4 nm was obtained. On the other hand, Peng used an alumina-based slurry with the same type of steel and reported that the oxidizer, oxidizer content and abrasive content were the most important factors affecting the polishing performance, material removal rate and the surface roughness<sup>41</sup>.

Jiang et al. conducted chemical mechanical polishing trials on AISI 52,100 steel using H<sub>2</sub>O<sub>2</sub> as the oxidizer and glycine as the complexing agent. As the H<sub>2</sub>O<sub>2</sub> concentration increased, the material removal rate (MRR) rapidly increased, followed by a gradual decrease and eventual stabilization<sup>42</sup>. Wu et al. performed CMP on AISI 52,100 steel using H<sub>2</sub>O<sub>2</sub> as the oxidizer and a TiSol-NH<sub>4</sub> dispersion as the complexing agent. Similarly, when the concentration of H<sub>2</sub>O<sub>2</sub> increased, the material removal rate (MRR) rapidly increased, followed by a gradual decrease, and eventually reached a stable point<sup>43</sup>. Zhao and colleagues utilized K<sub>2</sub>S<sub>2</sub>O<sub>8</sub> as the oxidizing agent to examine the polishing ability of GCr15 steel. The MRR increased nearly linearly as the concentration of K<sub>2</sub>S<sub>2</sub>O<sub>8</sub> increased. As previously stated, CMP of GCr15 steel relies on oxidation for its critical processes<sup>44</sup>.

Several commonly used techniques to alter the corrosion behavior of steel include surface treatments such as shot peening<sup>45</sup>, the use of inhibitors<sup>46,47</sup> and the use of surfactants with inhibitors<sup>48,49</sup>. Shot peening increases the surface roughness, which leads to an increased contact area; as a result, the resistance to corrosion decreases. Rivera et al.<sup>50</sup> used inhibitors to improve resistance to corrosion in an acidic medium and reported a significant improvement in corrosion resistance depending on the quality of the inhibitor. Abd-Elal<sup>51</sup> used surfactants with inhibitors to improve resistance to corrosion. Their results revealed greater inhibition efficiency under all the tested conditions.

CMP technology is considered a superior method that can fulfill both surface roughness and smoothness needs. It is now one of the most convenient technologies for processing hard and brittle materials to achieve a supersmooth and undamaged surface and is commonly utilized in large-scale integrated circuits, semiconductors, and various industrial processes. CMP is likely the best option for high-efficiency ultraprecision machining of large ultrathin stainless-steel flexible display substrate surfaces to achieve ultrasurface and undamaged machining surfaces<sup>52</sup>. However, the use of CMP as an alternative surface treatment for preventing the corrosion of metals has not been studied. The mechanism of silica nanoparticle removal during the CMP process is not yet well understood, especially in acidic mediums. CMP increases the surface smoothness, changes the surface wettability behavior and surface roughness and forms a protective layer on the surface. These substantial modifications to the surface properties are expected to significantly affect the corrosion resistance of metals. The formation of a durable protective layer decreases the surface roughness and improves the surface corrosion resistance.

In this study, an investigation of the effects of CMP on the surface properties of steel for its validation as a surface treatment for metals to improve the corrosion resistance was performed. A mechanically polished (MP) sample was used as the baseline, and the effect of the oxidizer in the CMP slurry on the surface properties was investigated in terms of wettability, surface roughness, material removal rate and static corrosion by immersing the samples in an acidic medium. The corrosion rates were measured from pre- and post- immersion weight differences. Moreover, potentiostatic and potentiodynamic analyses and Tafel plots were constructed to evaluate the effects of CMP on the electrochemical corrosion behavior of the steel.

Materials and methods

Materials

In this study, low-carbon steel from AL-AHDAB, an Iraqi oil field company, was utilized. The chemical composition is listed in Table 1. The samples were cut into 10×10 mm squares with a 2 mm thickness.

CMP experiments

Slurry and oxidizer

A commercial silica (SiO<sub>2</sub>)-based slurry with a solid loading of 10 wt%. with a particle size of 50 nm was obtained from BASF, SE, Germany, and used in the polishing experiments. The pH was adjusted with 0.1 M HCl/0.1 M NaOH, and the pH values were adjusted according to the isoelectric point of the silica nanoparticles to ensure stability during the polishing process. Hydrogen peroxide (H<sub>2</sub>O<sub>2</sub> 34.5–36.5 wt% obtained from Sigma Aldrich) was diluted to 3 wt% by adding deionized water (DIW).

The CMP experiments were performed with a SUBAIV-IC1000 stacked polishing pad on a desktop Tegrapol-31 polisher. The downforce during the experiments was set to 70 N on the 10×10×2 mm steel coupons. The rotational speed for both the turntable and the sample holder was set to 100 rpm. The CMP slurry was fed at a constant flow rate of 100 ml/min. The samples were mechanically polished with a FORCIPOL 1V, Metkan grinder-polisher using 800 μm silicon carbide (SiC) abrasive paper at 300 rpm for 3 min. All polishing experiments were conducted three times. The CMP performance was evaluated in terms of the MRR (Å/min), wettability and average surface roughness. The material removal rates were determined from the pre- and post-CMP weight differences these difference were measured using a high-precision balance with 0.01 mg accuracy.

Material removal rate (MRR)

The material removal rates obtained with the mechanically polished samples and two different CMP treatments (i.e., 10 wt% silica slurry and 10 wt% slurry + 3% H<sub>2</sub>O<sub>2</sub>) were evaluated by weighing the samples before and after CMP and mechanical polishing. Three samples of each type were polished for the average material removal rate (MRR) measurements. Equation (1)<sup>11</sup> below was used for the calculations:

MRR = (10^8 × Δm) / (7.98 × A × t) (1)

where MRR (Å/min) is the material removal rate, Δm (g) is the weight difference before and after the polishing process, A (cm<sup>2</sup>) is the area of the sample and t (minutes) is the polishing time.

Element	C	Si	Mn	P	S	Ni	Mo	Cr	Fe
%	0.10	0.269	0.616	0.003	0.001	0.050	0.106	0.653	98.13

Table 1. Chemical composition (wt%) of the steel sample.

## Surface characterization

### Hardness evaluation

Hardness testing of the steel samples (MP-baseline) and CMP-treated samples was conducted via the Vickers hardness testing protocol using an ARS9000 fully automatic micro hardness testing system (Future Teach, FM-300e, Kanagawa, Japan) with an applied load of 1000 g for 5 s. Three measurements of each sample were collected, and the average was reported.

### Characterization of the surface roughness

The average surface roughness ( $R_a$ ) of the steel samples was measured using a Dektak 6M stylus profilometer, following the ASME B46.1 standard, which is commonly used for surface roughness characterization. The surface roughness values were recorded as the average of three measurements per sample. Additionally, the surface topography of the steel samples after seven days of static corrosion in an acidic medium was examined using a ZEISS EVO/LS10 SEM.

### Wettability analyses

The steel samples were characterized for wettability via contact angle measurements with deionized water (DIW). The contact angles were measured via the sessile drop method using a KSV ATTENSION Theta Lite optical goniometer. The size of the drop was maintained at  $\sim 120 \mu\text{m}$ . The average of three tests performed for each sample at room temperature is reported.

## Immersion tests

The corrosion behavior was examined using immersion tests. The steel samples in each mechanical polishing treatment group and chemical mechanical polishing treatment group were suspended in glass beakers with DIW at pH 2 with the help of an insulated wire. After 7 days of exposure at room temperature, the samples were removed from the harsh environment, cleaned thoroughly with DIW, dried with air and weighed on a balance (Swiss Made ES125SM) with an accuracy of  $\pm 0.01 \text{ g}$ . The weight before and after performing the immersion test after every 24 h of exposure was used to determine the corrosion rate using the following Eq. (2)<sup>51</sup>:

$$T_c = \frac{8.76 * 10^4 * \Delta M_c}{\rho * A * t} \quad (2)$$

where  $T_c$  is the corrosion rate in mm/year,  $\Delta M_c$  is the mass loss in g,  $A$  is the area in  $\text{cm}^2$ ,  $t$  is the testing time in hours and  $\rho$  is the specific mass in  $\text{g/cm}^3$  ( $7.85 \text{ g/cm}^3$ ).

## Electrochemical analyses

The electrochemical corrosion behavior of the steel substrates was investigated via potentiostatic and potentiodynamic analyses in DIW at pH 2 at room temperature using a Gamry 1000 potentiostat. The electrochemical measurements were performed with a three-electrode glass cell consisting of a steel sample as the working electrode, a saturated calomel electrode (SCE) as the reference electrode, and a platinum helical wire as the counter electrode. The surface area exposed to the electrolyte was  $1 \text{ cm}^2$ . The potentiodynamic polarization curves were obtained with a scan rate of  $1 \text{ mV/s}$  from  $-0.6$  to  $1.5 \text{ V}$ . The time period for potentiostatic scanning was set to 1800 s with an input potential of  $0 \text{ V}$  vs.  $E_{\text{ref}}$ ; the real values shown during the test were  $\sim 90\text{--}100 \mu\text{V}$ , and these were considered to be negligible and assumed to be zero. The total volume of the electrolyte used was 200 ml.

## Results and discussion

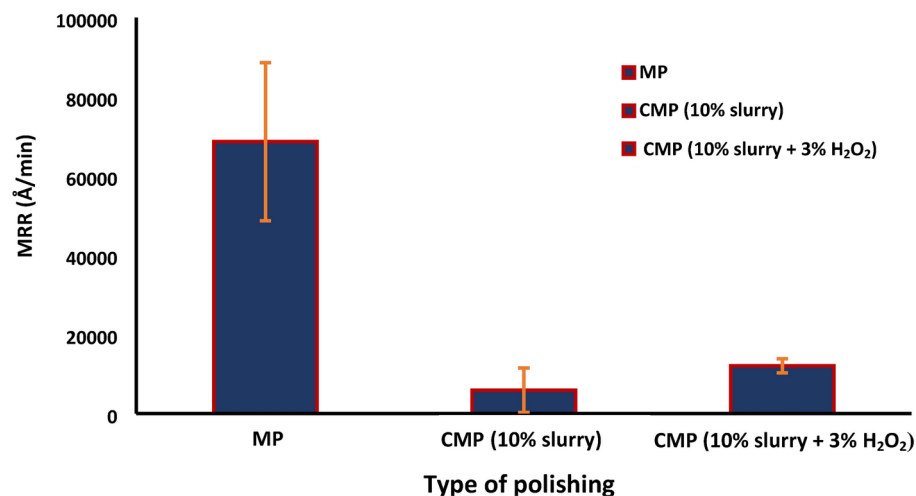
### Material removal rate evaluation

Figure 1 shows the material removal rates of the steel samples during three different surface treatments: (1) mechanical polishing, (2) CMP with a 10 wt% silica slurry and (3) CMP with 3%  $\text{H}_2\text{O}_2$  in a 10 wt% silica slurry. Among them, the MRR was greater after the MP treatment because of the mechanical polishing by the abrasive silicon carbide paper; this led to a very rough and grooved surface, as shown in Fig. 3a and b. The presence of  $\text{H}_2\text{O}_2$  in the slurry results in the formation of an oxide layer on the steel surface; this causes an increase in the MRR<sup>30,41</sup> since the removal of the oxide layer from the surface is easier than that from the pure material because of the mechanical action of the slurry particles (silica). Despite the increased MRR with an oxidizer in the slurry, the CMP process results in an increased smoothness. In the case of CMP without an oxidizer in the silica slurry, the material removal is accomplished predominantly by the mechanical abrasion of the silica abrasive on the steel surface, and the MRR is the lowest in this case among the three surface treatments<sup>30</sup>.

## Surface characterization

### Hardness measurements

The microhardness results for the steel samples are shown in Fig. 2. Compared with the MP process, the CMP process improved the hardness. The samples treated with CMP and an oxidizer in the slurry had the highest hardness values among the three surface treatments; these results could be attributed to an oxide film growth on the steel surface. The film formed on the steel surface in the presence of  $\text{H}_2\text{O}_2$  was composed of two layers. The outer layer was much stronger than the inner layer and the steel substrate; thus, these samples were harder than those for the other two cases<sup>52</sup>.



**Fig. 1.** Removal rates of the steel samples with different surface treatments.

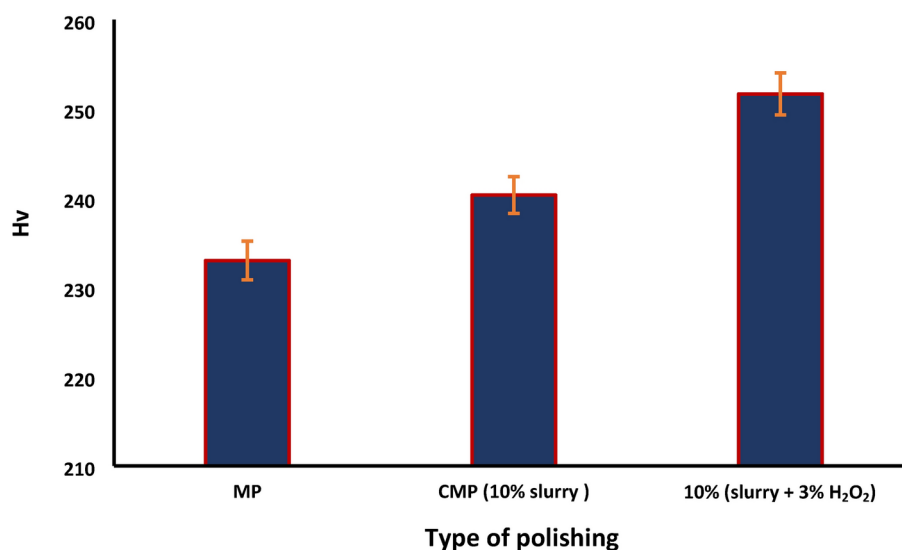
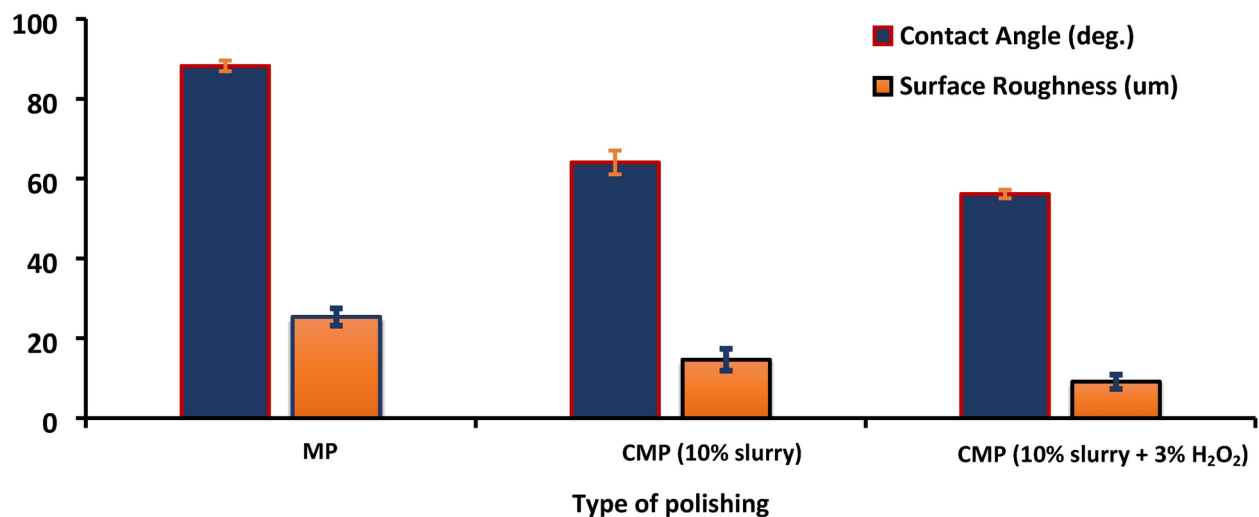


**Fig. 2.** Hardness measurements of the steel samples with different surface treatments.

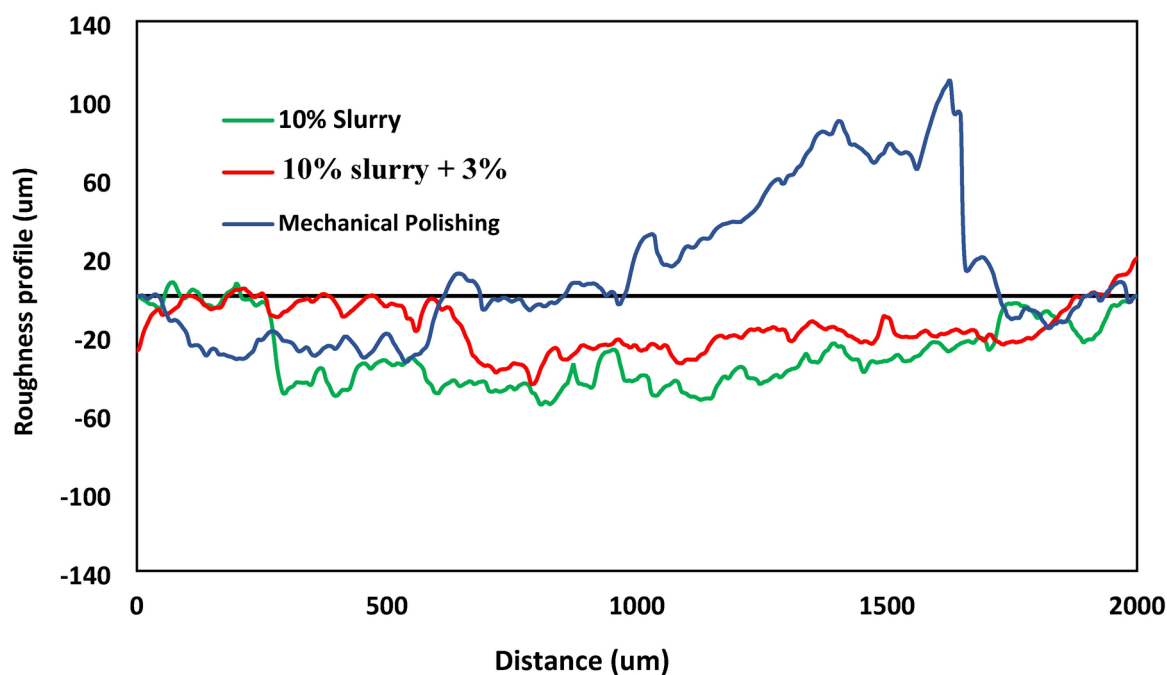
#### Surface roughness and wettability analyses

Figure 3 shows the average surface roughness as a function of the different surface treatment techniques. The mechanically polished sample was the baseline; the surface roughness of the mechanically polished sample was the highest among the three cases since it was polished with sandpaper (800  $\mu\text{m}$  SiC) and flowing DIW. Here, the samples treated with CMP and 3 wt% H<sub>2</sub>O<sub>2</sub> as an oxidizer in the silica slurry had the smoothest surface among the three cases.

The smooth surface from the CMP process with H<sub>2</sub>O<sub>2</sub> was caused by the formation of a protective oxide layer on the metal surface; this result was attributed to abrasion by the silica nanoparticles and the presence of an oxidizer in the slurry<sup>31,40</sup>. Moreover, the surface roughness profiles of the samples are shown in Fig. 3b; here, the CMP-treated samples in the presence of H<sub>2</sub>O<sub>2</sub> have fewer defects and surface scratches. Figure 3a shows the wettability behavior of steel samples after the three different surface treatments. The contact angle decreased when the surface became smoother; thus, the samples that were chemically and mechanically polished with 10% slurry + 3% H<sub>2</sub>O<sub>2</sub> had greater wettability than the other samples. Thus, the presence of the oxidizer in the silica slurry increased the contact area between the steel surface and the droplet, which resulted in a small contact angle. Moreover, the roughness of the steel surface caused by mechanical polishing led to scratches and pits on the surface due to the action of the silicon carbide granules; these scratches and pits clearly affected the contact angle between the drop and the surface.



a. Surface wettability and average roughness (Ra) values for the different surface treatments.



b. Average roughness profile at different surface treatments after 7 days of immersion.

**Fig. 3.** (a) Surface wettability and average roughness (Ra) values for the different surface treatments. (b) Average roughness profile at different surface treatments after 7 days of immersion.

### Immersion tests

The effect of 7 days of immersion on the corrosion rate is shown in Fig. 4. For the first two days, elevated corrosion rates were observed, and the rates decreased as time increased. This decrease was caused by an increase in the formation of the corrosion products over time. Since the immersion tests were conducted under static conditions, a thick layer grew over time; thus, the corrosion rate decreased<sup>53</sup>, and the mechanically polished samples corroded at higher rates than the CMP-treated samples. This occurred because of the effectiveness of the acidic medium in the first days of immersion; additionally, the layer formed on the mechanically treated surface broke down more quickly than the other surfaces. The decreased corrosion rates of the CMP-treated samples could be attributed to the formation of a protective oxide film due to the presence of an oxidizer in the slurry, i.e., (10% silica slurry + 3% H<sub>2</sub>O<sub>2</sub>) and a smoother surface with respect to the CMP-treated sample with 10% silica without an oxidizer. The use of an oxidizer in the silica slurry provided a high removal rate, a flat surface and high smoothness; thus the defects that caused corrosion were controlled. As a result, the corrosion rate decreased, and



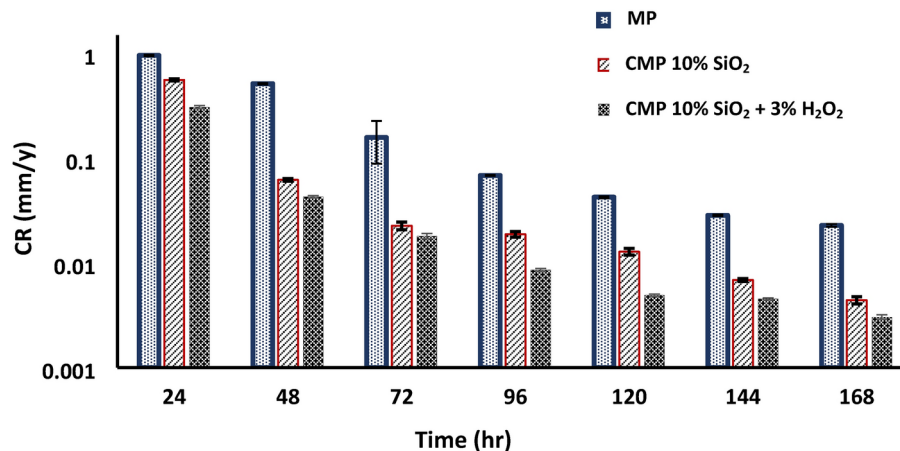


**Fig. 4.** Relationship between the corrosion rate and immersion time for 7 days.

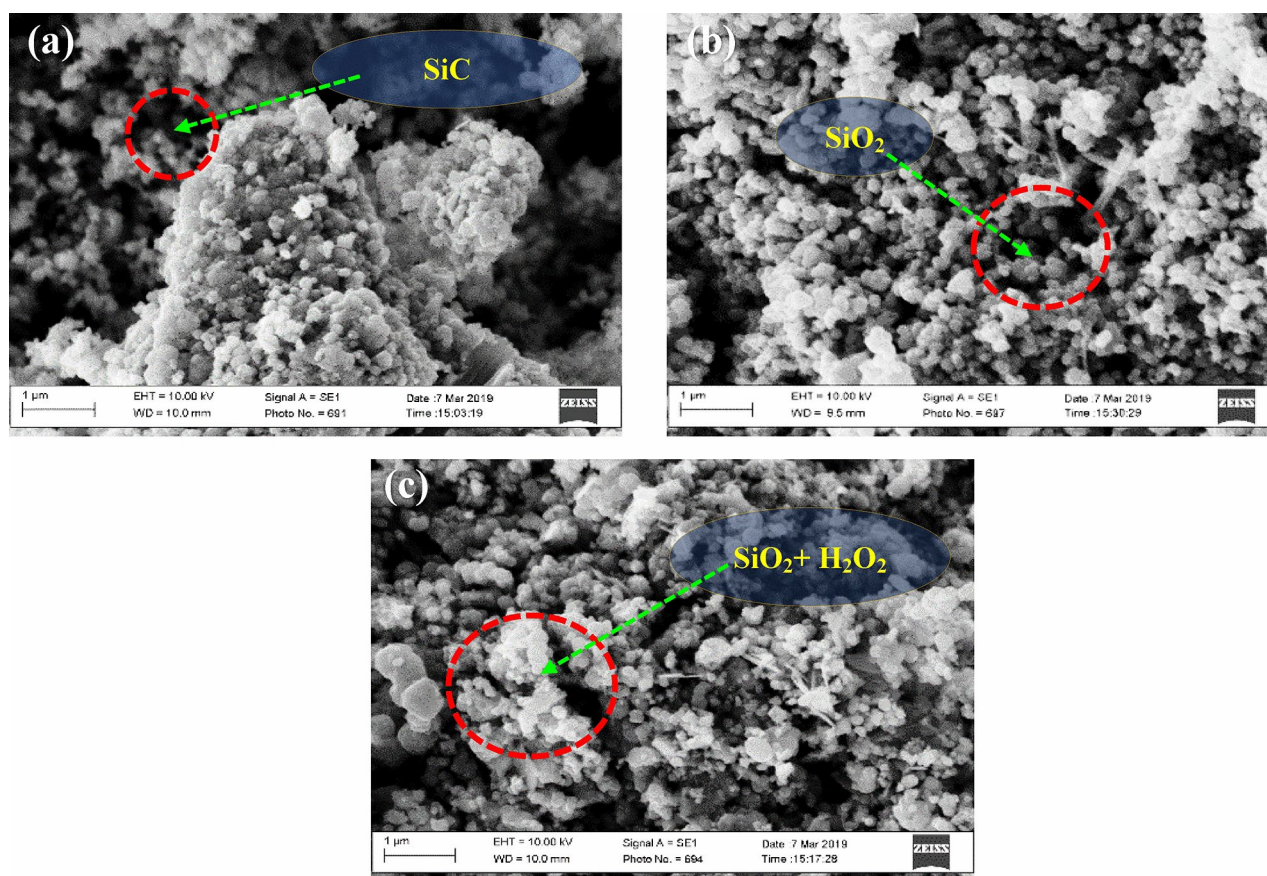


**Fig. 5.** SEM images of the steel samples after seven days of immersion tests: (a) mechanically polished, (b) CMP with 10 wt% slurry + no oxidizer and (c) CMP with 10 wt% slurry + 3 wt% H<sub>2</sub>O<sub>2</sub>.

this effect continued over time. This result highlights the importance of using chemical-mechanical polishing as an alternative method to avoid corrosion.

The adhesion of the silica to and adsorption of hydrogen peroxide on, the post-polished steel surfaces in the three environments were observed using SEM. The SEM image of the mechanically polished steel substrate revealed wells and protrusions; this involved deep scratches and indicated a rough surface, as shown in Fig. 5a. After CMP with the silica-based slurry (10 wt%), the polished surface had fewer deep scratches and few abrasions due to the nature of the nanoparticles, which led to their adhesion to the steel surface. Numerous silica particles were present on the steel surface, as shown in Fig. 5b. Figure 5c shows the SEM image of the steel sample treated

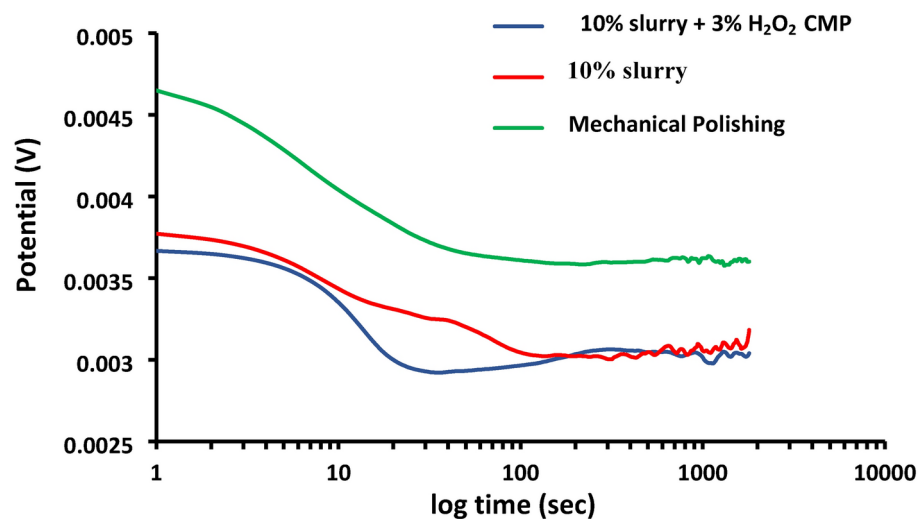


Fig. 6. Potentiostatic scans ( $I_m$  vs. time) of the steel samples subjected to different surface treatments.

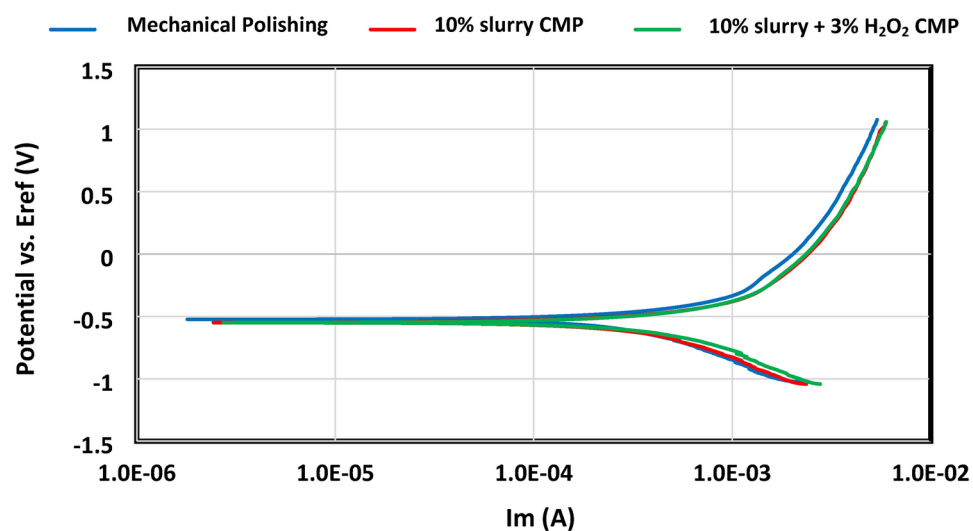


Fig. 7. Potentiodynamic polarization curves of the steel samples subjected to different surface treatments.

with the silica-based slurry and  $H_2O_2$ . Many silica particles adhered to the steel surface. As a result, the polishing performance of the steel surface, including its surface roughness and MRR, depended on the oxidizer content in the slurry; thus, the presence of the oxidizer in the silica slurry improved the abrasion of the slurry on the steel substrate and led to the adhesion of the silica particles to the steel surface.

### Electrochemical analyses

The evolution of the potentiostatic scan with respect to time under different surface treatments in an acidic medium ( $pH = 2$ ) is shown in Fig. 6. All curves initially showed a decrease in potential followed by a stabilization period, which could be attributed to the formation of an oxide film covering the substrate surface<sup>54</sup>. The MP-samples initially had a high potential, and the potential then decreased with respect to time; thus, the oxide layer formation needed an extended amount of time, and the sample corroded rapidly. The samples subjected to CMP with a 10 wt% slurry + no oxidizer and CMP with a 10 wt% slurry + 3 wt%  $H_2O_2$  showed different behaviors; this was evident from the lower potential, which clearly reflected the effects of the additives. In addition, the potency gradually decreased with time; thus result indicated that a protective layer formed on the surface. This behavior could also be shown by potentiodynamic tests.

Potentiodynamic polarization curves were obtained after 45 min of immersion in an acidic solution at a  $pH$  of 2. The corresponding corrosion current densities " $I_{corr}$ " obtained via Tafel extrapolation are depicted in Fig. 7, and the data are listed in Table 2. Equation (3) was used to calculate  $I_{corr}$ , as shown below<sup>55</sup>:



Polishing	CR(mpy)	Corrosion rate (mm/yr)	$I_{corr}$ (mA/cm <sup>2</sup> )	$E_{corr}$ (mv)	$\beta_A$ (V/decade)	$\beta_C$ (V/decade)
Mechanical polishing	17e-3	0.7	37e-3	- 525	56	41
CMP 10 wt% Slurry	11e-3	0.5	23e-3	- 549	48	18
CMP (10 wt% Slurry + 3% H <sub>2</sub> O <sub>2</sub> )	7e-3	0.3	15e-3	- 550	2	7

**Table 2.** Tafel plot data of the steel samples obtained via potentiodynamic data analyses.

$$I_{corr} = \frac{\beta_a}{2.3(\beta_a + \beta_c)} \frac{\Delta I}{\Delta E} \quad (3)$$

The corrosion rate was calculated using the following formula<sup>56</sup>:

$$Corrosion\ rate = \frac{0.13 I_{corr} (E.W)}{density} \quad (4)$$

where EW is the equivalent weight,  $I_{corr}$  is the current density in  $\mu\text{A}/\text{cm}^2$ , density is the density of the corroding species in  $\text{g}/\text{cm}^3$ , and  $\frac{\Delta I}{\Delta E}$  is the slope of the polarization resistance plot, where  $\Delta E$  is expressed in volts and  $\Delta I$  is expressed in  $\mu\text{A}$ . Note that all these data and calculations ( $I_{corr}$ ,  $E_{corr}$ ,  $\beta_A$ ,  $\beta_C$ , corrosion rate) are obtained using the Gamry 1000 potentiostat software.

Since the medium utilized as the electrolyte for the potentiodynamic tests was acidic and the anodic potential was higher than the cathodic potential for the samples that underwent MP and CMP with a 10 wt% silica slurry, the corrosion rate increased. However, for samples treated with CMP with 10 wt% silica slurry + 3 wt% H<sub>2</sub>O<sub>2</sub>, the cathodic potential was higher than the anodic potential; hence, decreased corrosion rates were observed. Specifically, the corrosion current density of the steel samples treated with CMP decreased from  $23\text{e}^{-3} \text{ mA}/\text{cm}^2$  in the absence of the oxidizer to  $15\text{e}^{-3} \text{ mA}/\text{cm}^2$  in the presence of the oxidizer. Among the three surface treatments, the current found for the MP samples had the highest value of  $37\text{e}^{-3} \text{ mA}/\text{cm}^2$ , whereas the CMP samples (10 wt% slurry + 3% H<sub>2</sub>O<sub>2</sub>) had the lowest value of  $15\text{e}^{-3}$ . The current of the MP was directly related to the corrosion rates of the samples. However, the current of CMP in the presence of the oxidizer enhanced the corrosion resistance of the steel surface because the protective layer formed on the surface prevented the medium from penetrating the metal surface. The corrosion rates (mm/y) presented in Table 2 showed a similar trend as the corrosion rates obtained from the static corrosion tests, as shown in Fig. 4.

The improvement in corrosion resistance observed after chemical mechanical polishing (CMP) is attributed to a combination of mechanical surface modification and chemical passivation. The CMP process removes surface irregularities, reducing micro-defects and roughness that typically serve as initiation sites for localized corrosion. The presence of an oxidizer (H<sub>2</sub>O<sub>2</sub>) in the CMP slurry plays a crucial role by promoting the formation of a stable oxide layer on the steel surface. This oxide layer not only enhances corrosion resistance by acting as a protective barrier but also contributes to increased surface hardness due to its densification. Furthermore, the smoother surface achieved through CMP reduces the adhesion of corrosive species and minimizes localized electrochemical reactions, thereby lowering overall corrosion rates. The wettability analysis further supports this mechanism, as the polished surface exhibited improved hydrophilicity, which facilitates a more uniform distribution of the corrosive medium, reducing the risk of localized attack. The combined effects of oxide layer formation, increased hardness, and surface smoothness result in a more corrosion-resistant steel surface, as confirmed by both static and electrochemical corrosion tests.

## Conclusion

The corrosion behavior of carbon steel in a harsh medium after mechanical and chemical mechanical polishing treatment has been reported. Based on these findings, the combination of an oxidizer (H<sub>2</sub>O<sub>2</sub>) and silica nanoparticles (SiO<sub>2</sub>) in the CMP slurry strongly affected the average roughness and enhanced the material removal rate. The presence of oxidizers in the polishing slurry resulted in the oxide layer formation on the surface, which was easier to abrade than steel. However, after the CMP process, the oxide layer served as a protective layer against corrosion. CMP with silica nanoparticles in the slurry resulted in smoother surfaces than those produced by pure mechanical polishing. The combined effect of the silica nanoparticles and oxidizers in the slurry removed the protruded parts from the surface and fills the valleys, resulting in a durable and corrosion-resistant surface. On the basis of these data, the chemical-mechanical polishing process, as an alternative method to reduce or limit corrosion, was effective in aquatic environments and could be reliable in industrial applications. The corrosion rate determined after seven days of immersion tests showed that roughness and wettability played important roles in corrosion. In addition, the behavior between the immersion test and the electrochemical corrosion test was consistent. The decreased wettability and increased smoothness of the chemically mechanically polished surface resulted in better corrosion resistance than that of the rough baseline surface prepared with pure mechanical polishing. The mechanical action of the silica particles caused damage to the surface, and this damage led to an increase in the corrosion rate.

## Data availability

The datasets generated and analysed during the current study are available from the corresponding author on reasonable request.

Received: 31 July 2024; Accepted: 10 April 2025

Published online: 30 April 2025

## References

1. Jasim, Z. I., Rashid, K. H. & Khadom, A. A. Study of chemical reactions in applied chemistry. *Russ. J. Appl. Chem.*, **6** (2024).
2. Jasim, Z. I. et al. Bio tribocorrosion behavior of metallic materials. *J. Bio Tribol. Corros.* <https://doi.org/10.1007/s40735-023-00783-4> (2023).
3. Al-Azawi, K. F., Ahmed, Z. W., Ali, E. H., Khadom, A. A., Abraham, H. H. & Rashid, K. H. Investigations on corrosion resistance of metal alloys. *Results Chem.* **5** (2023).
4. Sedlacek, V. *Metallic Surfaces, Films, and Coatings* 25 (Elsevier, 1992).
5. Sudesh, T. L., Wijesighe, L. & Blackwood, D. J. Surface characteristics of materials in tribology. *J. Phys. Conf. Ser.* **28**, 74–78 (2006).
6. Jargelius-Pettersson, R. F. A. Electrochemical studies on surface coatings. *J. Electrochem. Soc.* **145**, 1462 (1998).
7. Silva, L. R., Corrêa, E. C. S., Brandão, J. R. & de Ávila, R. F. Cleaner production and surface treatments. *J. Clean. Prod.* **256**, 103287 (2020).
8. Lou, S. et al. Design and applications of surface materials in engineering. *Mater. Des.* **104**, 320–326 (2016).
9. Fredj, N. B., Nasr, M. B., Rhouma, A. B., Braham, C. & Sidhom, H. Properties and performance of materials under mechanical stress. *J. Mater. Eng. Perform.* **13**, 564–574 (2004).
10. Rhouma, A. B. et al. Advanced manufacturing techniques and material performance. *Int. J. Adv. Manuf. Technol.* **105**, 1699–1711 (2019).
11. Cook, L. M. Chemical processes in glass polishing. *J. Non-Cryst. Solids* **120**(1–3), 152–171 (1990).
12. Lyon, K. N., Marrow, T. J. & Lyon, S. B. Material processing technologies for high precision. *J. Mater. Process. Technol.* **218**, 32–37 (2015).
13. Ghosh, S. & Kain, V. Nuclear materials and their tribological properties. *J. Nucl. Mater.* **403**, 62–67 (2010).
14. Li, L. F. et al. Corrosion science and its impact on material longevity. *Corros. Sci.* **47**(5), 1307 (2005).
15. Rhouma, A. B., Sidhom, H., Braham, C., Lédion, J. & Fitzpatrick, M. E. Surface engineering for improved material durability. *J. Mater. Eng. Perform.* **10**(5), 507 (2001).
16. Zhao, H., Van Humbeeck, J., Sohler, J. & De Scheerder, I. Material science in medical device engineering. *J. Mater. Sci. Mater. Med.* **13**(10), 911 (2002).
17. Fajnor, P., Liptáková, T. & Konstantová, V. Material engineering for environmental applications. *Mater. Eng.* **17**(3), 21 (2010).
18. Zatkaliková, V. & Liptáková, T. Research advances in material engineering. *Mater. Eng.* **18**(4), 115 (2011).
19. He, X. et al. Friction and wear behavior of materials. *Friction* **1**(4), 327 (2013).
20. Jiang, L., He, Y. & Luo, J. Tribological behavior of materials in different conditions. *Tribol. Lett.* **56**(2), 327 (2014).
21. Li, Y. (ed.) *Microelectronic Applications of Chemical Mechanical Planarization* (Wiley, 2008).
22. Zhang, W. & Lei, H. Analysis of material wear and friction resistance. *Friction* **1**(4), 359 (2013).
23. Zhao, D. & Lu, X. Tribological properties of materials under dynamic loads. *Friction* **1**(4), 306 (2013).
24. Nagaoka, S. et al. Thin film materials in tribology. *Thin Solid Films* **576**, 31–37 (2015).
25. Zhu, H. et al. Surface science applications in materials engineering. *Appl. Surf. Sci.* **236**, 120–130 (2004).
26. Zantye, P. B., Kumar, A. & Sikder, A. Material science in advanced tribology. *Mater. Sci. Eng. R Rep.* **45**, 89–220 (2004).
27. Li, X. et al. Advanced photovoltaic materials. *Nat. Chem.* **7**, 703–711 (2015).
28. Lei, H. & Luo, J. Wear and surface engineering. *Wear* **257**, 461–470 (2004).
29. Seo, Y. J. & Lee, W. S. Materials engineering in tribology. *Mater. Sci. Eng. B* **118**, 281–284 (2005).
30. Hu, X. et al. Friction and wear on different materials. *Appl. Surf. Sci.* **258**(15), 5798 (2012).
31. Lee, S. J. et al. Material engineering for corrosion resistance. *J. Alloys Compd.* **558**, 95 (2013).
32. Lee, D., Lee, H. & Jeong, H. Precision engineering in manufacturing. *Int. J. Precis. Eng. Manuf.* **17**, 1751–1762 (2016).
33. Biemann, M., Mahajan, U., Singh, R. K., Agarwal, P., Mischler, S., Rosset, E. & Landolt, D. Corrosion and material performance. *MRS Online Proc. Libr.*, **556** (1999).
34. Mischler, S. Tribology and corrosion studies. *Tribol. Int.* **41**(7), 573 (2008).
35. Stojadinović, J., Bouvet, D., Declercq, M. & Mischler, S. Materials in tribology and surface engineering. *Tribol. Int.* **42**(4), 575 (2009).
36. Ziomek-Moroz, M., Miller, A., Hawk, J., Cadien, K. & Li, D. Y. Wear mechanisms in advanced materials. *Wear* **255**(7–12), 869 (2003).
37. Collman, J. P., Kubota, M. & Hosking, J. W. Electrochemical behavior of metal complexes. *J. Am. Chem. Soc.* **89**(18), 4809 (1967).
38. Du, T., Vijayakumar, A. & Desai, V. Electrochemical studies on corrosion. *Electrochim. Acta* **49**(25), 4505 (2004).
39. Lee, J. O., Park, G., Park, J., Cho, Y. & Lee, C. K. Precision engineering in manufacturing processes. *Int. J. Precis. Eng. Manuf.* **16**(7), 1229 (2015).
40. Kao, M. J.; Hsu, F. C.; Peng, D. X. Advanced materials science and engineering. *Adv. Mater. Sci. Eng.* **8**. (2014).
41. Peng, D. X. Tribology and industrial lubrication. *Ind. Lubr. Tribol.* **66**, 124 (2014).
42. Jiang, L., He, Y. & Luo, J. Surface science and tribology. *Appl. Surf. Sci.* **330**, 487–495 (2015).
43. Wu, H. et al. Tribological behavior of composite materials. *Tribol. Lett.* **68**, 34 (2020).
44. Zhao, T. et al. Electrochemical studies in material science. *J. Appl. Electrochem.* **51**, 803–814 (2021).
45. Peltz, J. D. S., Beltrami, L. V. R., Kunst, S. R., Brandolt, C. & Malfatti, C. D. F. Material research in surface engineering. *Mater. Res.* **18**(3), 538 (2015).
46. Rivera-Grau, L. M. et al. Electrochemical and material science. *Int. J. Electrochem. Sci.* **8**(2), 2491 (2013).
47. Yıldız, R., Döner, A., Doğan, T. & Dehri, I. Corrosion science in modern engineering. *Corros. Sci.* **82**, 125 (2014).
48. Abd-Elaal, A. A., Shaban, S. M. & Tawfik, S. M. Tribology in engineering applications. *J. Assoc. Arab Univ. Basic Appl. Sci.* **24**(1), 54 (2017).
49. Hu, X. et al. Material surface engineering. *Appl. Surf. Sci.* **258**, 5798–5802 (2012).
50. Aiad, I., Shaban, M. S., Elged, H. A. & Aljoboury, H. O. Petroleum and material engineering. *Egypt. J. Pet.* **27**(4), 877 (2018).
51. ASTM Committee G-1 on Corrosion of Metals. (ASTM International, 2017).
52. Liu, J., Jiang, L., Deng, C., Du, W. & Qian, L. J. F. Friction behavior of tribological materials. *Friction* **6**(3), 307 (2018).
53. Slaimana, Q. J. & Hasan, B. O. Chemical engineering studies in tribology. *Can. J. Chem. Eng.* **88**(6), 1114 (2010).
54. Hamlaoui, Y. et al. Material science in tribology. *Mater. Chem. Phys.* **113**(2–3), 650 (2009).
55. Instruments, G. I. G. *Warminster* (PA, 2011).
56. Denny, A. J. *Principles and Prevention of Corrosion* (Pearson-Prentice Hall: Upper Saddle River, 1992).

## Acknowledgements

The authors would like to acknowledge the Ministry of Oil and AL ALAHDAB Company in Iraq for preparing the steel samples. Special thanks to Assistant Prof. Dr. Ozgur Ertunc for his technical help.

## Author contributions

Conceptualization: Mohamed Ahmed; Formal analysis: Mohamed Ahmed , Maha Al-Ali , Ghassan H Abdullah ,Safa Khalaf Atiyaha , Ahmed Yaseen Ali Aljanabi ; Investigation: Mohamed Ahmed; Methodology: Mohamed Ahmed; Writing—original draft: Mohamed Ahmed; Scientific review: Buthainah Ali Al-Timimi and Maizirwan Mel.

## Declarations

## Competing interests

The authors declare no competing interests.

## Additional information

**Supplementary Information** The online version contains supplementary material available at <https://doi.org/10.1038/s41598-025-98210-w>.

**Correspondence** and requests for materials should be addressed to M.A. or B.A.-T.

**Reprints and permissions information** is available at [www.nature.com/reprints](http://www.nature.com/reprints).

**Publisher's note** Springer Nature remains neutral with regard to jurisdictional claims in published maps and institutional affiliations.

**Open Access** This article is licensed under a Creative Commons Attribution-NonCommercial-NoDerivatives 4.0 International License, which permits any non-commercial use, sharing, distribution and reproduction in any medium or format, as long as you give appropriate credit to the original author(s) and the source, provide a link to the Creative Commons licence, and indicate if you modified the licensed material. You do not have permission under this licence to share adapted material derived from this article or parts of it. The images or other third party material in this article are included in the article's Creative Commons licence, unless indicated otherwise in a credit line to the material. If material is not included in the article's Creative Commons licence and your intended use is not permitted by statutory regulation or exceeds the permitted use, you will need to obtain permission directly from the copyright holder. To view a copy of this licence, visit <http://creativecommons.org/licenses/by-nc-nd/4.0/>.

© The Author(s) 2025